Available online at www.sciencedirect.com

ScienceDirect

Procedia Engineering 191 (2017) 838 – 845

Procedia Engineering

www.elsevier.com/locate/procedia

Symposium of the International Society for Rock Mechanics

Identification of Rock Slope Discontinuity Sets from Laser Scanner and Photogrammetric Point Clouds: a Comparative Analysis

A. Riquelme[a]*, M. Cano[a], R. Tomás[a], A. Abellán[b]

[a]*Civil Engineering Department, University of Alicante, Alicante 03690, Spain*
[b]*Scott Polar Research Institute, Geography Department, University of Cambridge, England*

Abstract

Discontinuities play a key role in the mechanical, hydraulic and deformational behaviour of rock masses, frequently having a considerable influence on the stability of rock slopes. They can be characterized by several geometric parameters as the orientation, persistence, spacing, etc. Although orientation has been traditionally measured through well-known techniques as a compass, more recent remote sensing techniques such as 3D laser scanning allow deriving both strike and dip direction of discontinuities. The novel SfM (Structure from Motion) technique, which is much less expensive than 3D laser scanning, is becoming mainstream within the research community. This paper examines the generation of 3D point clouds of a rock slope obtained from both, 3D laser scanning and SfM techniques, and their application to the extraction of the orientations of the main discontinuity sets. To this aim, a selected sector from a cretaceous sedimentary rock cut slope placed in Alicante (Spain) is analyzed using both photogrammetric and terrestrial laser scanner (TLS) point clouds. Using ground control points extracted from printed targets scanned by means of TLS provided very accurate coordinates. As a result of this, the obtained adjustment error was minor than 3 mm. The comparison of the resulting point clouds shows a good correlation when the surface is orthogonal to the line of sight. On the contrary, the SfM dataset showed inaccuracies on sub-horizontal and oblique surfaces. Finally, a geometrical analysis was performed by means of DSE software. Three discontinuity sets were extracted from both point clouds. However, one more was extracted from the TLS dataset, but not from the SfM dataset.

Peer-review under responsibility of the organizing committee of EUROCK 2017

Keywords: SfM; LiDAR; rock mass; discontinuity; orientation

* Corresponding author. Tel.: 34-965-903-707; fax: +34-965-903-678.
E-mail address: ariquelme@ua.es

Peer-review under responsibility of the organizing committee of EUROCK 2017
doi:10.1016/j.proeng.2017.05.251

1. Introduction

Characterization of rock masses requires the acquisition of information, which has traditionally been collected by means of fieldwork, using a compass and a tape. Collection of data by means of fieldwork is a time consumption process, and the data quality may be affected by the user's experience [1]. Currently, different remote sensing techniques, such as 3D laser scanning or Structure from Motion (SfM) are being developed and becoming mainstream [2]. These techniques allow the acquisition of millions of points of a surface with high accuracy, and thus, the surface of a rock slope is digitalized by means of this dataset. As this dataset represents the surface of the slope, it may allow the identification and extraction of the existing discontinuity sets, its orientations [3–8], the normal spacing [9, 10], the persistence [11, 12] and the roughness [13], if the point cloud has enough quality.

The acquisition of 3D point clouds is, at present, mainly performed by means of two remote sensing techniques: 3D laser scanning and digital photogrammetry (such as stereographic image pairs or SfM). The instrument 3D laser scanner can be classified depending on its platform: aerial, terrestrial, mobile, off-shore, etc. In this work, the ground based laser scanner or Terrestrial Laser Scanner (TLS) is used. This instrument allows the acquisition of high resolution (density of points up to 10,000 point m^{-2}) and high accuracy (std. dev. < 1 cm at 100 m) 3D information of the ground surface. These instruments allow obtaining the coordinates (X, Y, and Z) of the points of a surface at high speed (more than 222,000 measurements per second) from a considerable distance of acquisition (up to 6,000 m). Nevertheless, the cost of acquisition of this instrument is currently expensive. The second technique, SfM, requires the use of a digital camera and a computer in order to process all digital photographs, and its precision is only limited by the camera resolution [14].However, this technique is cheaper than TLS.

TLS systems provide a 3D point cloud, which is usually automatically scaled. This allows the measurement of lengths, areas and volumes. Some instruments can be levelled by the user, so the point cloud is aligned respect a vertical axis. As a result, it is possible to measure dips of exposed planes. In addition to this, the point cloud can be oriented with respect to the north by means of a simply rotation with respect to the vertical axis OZ. This result leads to the possibility of obtaining the orientations (i.e. the dip direction and the dip) of the exposed planes and compare this measurement with those obtained by using a compass. On the contrary, the SfM technique requires the use of Ground Control Points (GCP) in order to scale, orient and correct the imagery distortions. 3D point clouds generated using both techniques have been used for the extraction of discontinuity sets [15], despite the fact that both point clouds present differences.

The present work analyses the extraction of the discontinuity sets of a rock slope using 3D point clouds, obtained by means of a TLS and SfM techniques, where the GCP are extracted from the TLS dataset by means of printed targets. The use of GCP extracted from targets by means of TLS is currently being applied in other researches [16]. First, the rock slope was scanned using the TLS. Then, the digital photographs were captured. The SfM process was performed using 6 GCP, which consisted of printed targets that had been placed on the rock surface. A sector was then cropped and the distances between those two models were computed, allowing the identification of those areas where the reconstructed surface showed differences. Finally, the discontinuity sets were extracted using both 3D point clouds, and the results were compared. This methodology is applied on a case of study which has previously been analyzed, using TLS datasets [17] and SfM datasets [15].

2. Case of study

This case of study consists of a rocky slope, located in Alicante (SE Spain), and formed by different levels of marls, argillaceous limestones and calcareous limestones (Fig. 1a) [18]. A preliminary observation of the rock slope shows that: (a) most of the discontinuities are smoothed by weathering, (b) the strata is slightly folded and has been affected by several normal faults, and (c) the sub-horizontal surfaces are partially (or even completely) covered by debris. In order to extract the discontinuity sets of the rock mass, a representative sector has been selected to minimize these mentioned effects that can mask the discontinuity surfaces. This sector is approximately located at the coordinates (717,640; 4,248,650; 75) (ETRS-89).

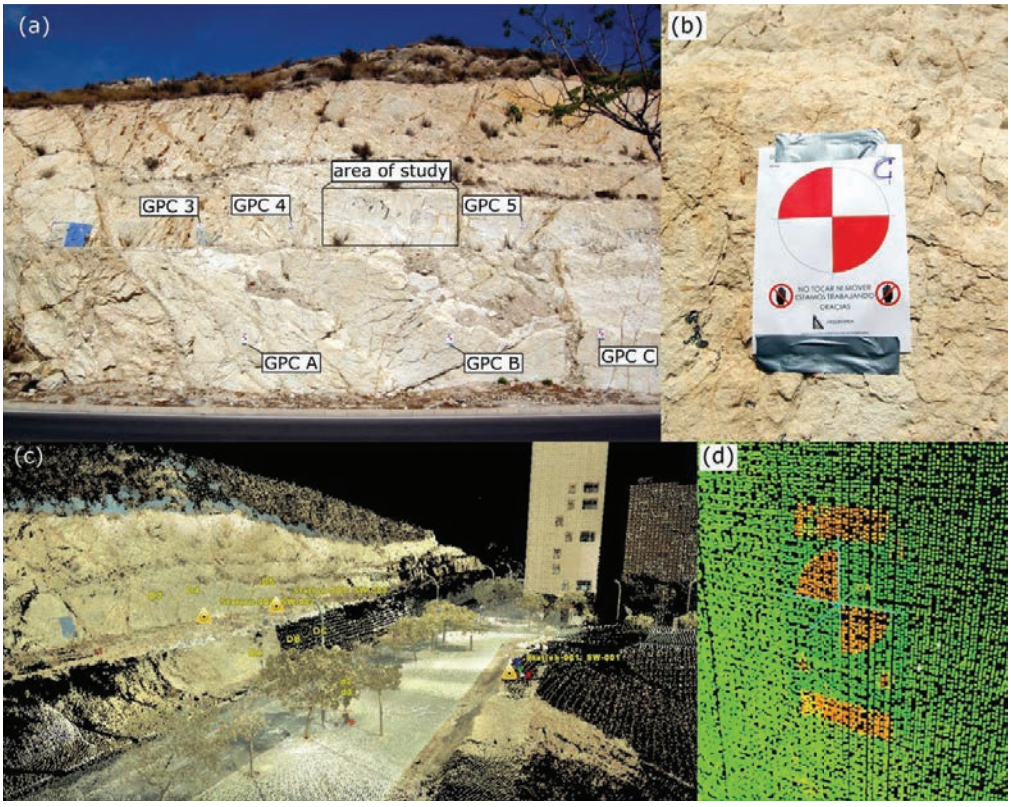

Fig.1. (a) Site view; (b) detail of a GPC; (c) point cloud view of the registered scans; (d) extraction of the coordinates of a target.

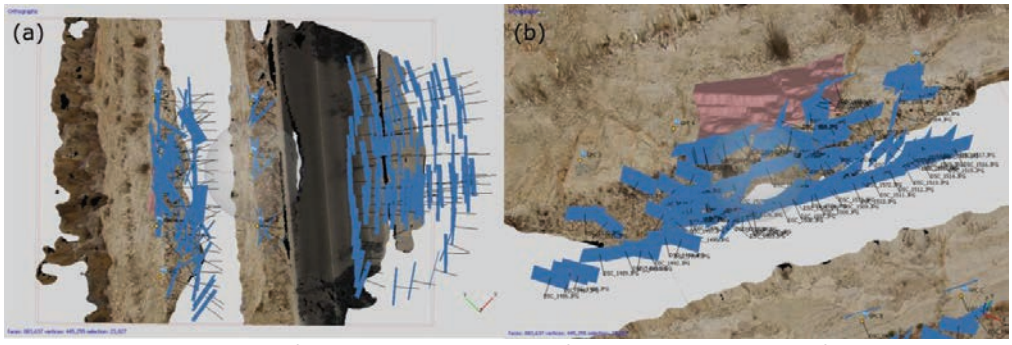

Fig. 2. (a) Top view of all camera locations; (b) detail of the cameras close to the area of interest.

3. Methodology

The followed methodology was based on two phases:

- Fieldwork data acquisition;
- Processing of the datasets and digital photographs.

3.1. Fieldwork data acquisition

Table 1. RMSE of the GCP in mm.

Label	X error	Y error	Z error	Total	Image (pix)
GPC C	-0.529458	-2.57569	0.880452	2.77303	0.016 (12)
GPC B	-2.41119	1.39405	0.364958	2.80898	0.046 (5)
GPC A	-0.171592	-0.143768	-0.411922	0.46882	0.011 (6)
GPC 4	-0.111419	2.33868	0.107771	2.34381	0.087 (18)
GPC 5	1.57512	2.75736	0.114717	3.17761	0.023 (10)
GPC 3	1.69761	-3.87487	-1.08401	4.3671	0.122 (6)
Total	**1.38437**	**2.47269**	**0.61616**	**2.90006**	**0.066**

Firstly, it is needed to inspect the rock slope in order to select the sector to be analyzed. Secondly, several printed targets are placed on sub-vertical planes, surrounding the area of interest. These targets consist of a circle divided in four equal sectors, where two opposite sectors have been coloured in red and the others are left in blank (Fig. 1b and d). Targets are evenly distributed on the rock slope around the sector to analyze (Fig. 1a). Then, the rock slope is scanned with a 3D laser scanner. In order to avoid occlusions as well as other biases, it is recommended to perform several stations from different points of view, and then register those scans [19].

In this work, a TLS model Leica C10 was used. In order to perform the registration process accurately, three 6″ circular targets were used. Each scan was performed in two steps. Firstly, for each scan station, the full sphere was scanned, setting the resolution to low. This process scanned all visible points from the scan station, and thus, all visible buildings and roads. Secondly, the sector to analyze was scanned in high resolution from the same position. Fig. 1c shows the result of the registration of the three scan stations.

Finally, digital photographs were captured following certain recommendations [20, 21]. It was used a camera model Nikon D50 (18 mm), setting a resolution of 3008×2000 and focal length equal to 18 mm. During this process, 198 digital photographs were captured. Fig. 2 shows all cameras locations as well as the inserted GPC.

3.2. Research work

The registered point cloud obtained using the TLS is defined in a local coordinate system. At this point, it is possible to align the point cloud with respect to the north using a virtual scanline, or simply using points acquired by means of topography. In this work, a simply way was used for registering the point cloud to the global coordinate system ETRS89. The project Plan Nacional de Ortofoto Aérea (PNOA), which is directed by the Instituto Geográfico Nacional (IGN), distributes a georeferenced 3DPC of Spain, acquired by means of an Aerial Laser Scanner (ALS). Using this reference, the TLS point cloud was aligned using the scanned buildings and the terrain.

The SfM process requires the use of GCP. In this case, the GCP were the printed targets which were placed on the rock slope. These targets were scanned during the TLS scanning process. As these targets have previously been registered, their center coordinates were extracted by means of the software Cyclone [22] (Fig. 1d). Each GCP was added to each digital photograph on its corresponding pixel. Then, the bundle adjustment was performed and the dense cloud was generated by means of the software Agisoft Photoscan Professional Edition [23].

The area of interest was then selected and cropped using the software CloudCompare [24]. The result of this process was two point clouds (TLS and SfM) of the same area. As both point clouds obtained with different methods were georeferenced in a global coordinate system, a direct comparison could be performed. This process leaded to the estimation of the quality of both models.

Finally, the discontinuity sets were extracted separately using the open-source software Discontinuity Set Extractor (DSE) [25], which is based on the method proposed by Riquelme et al. [4].

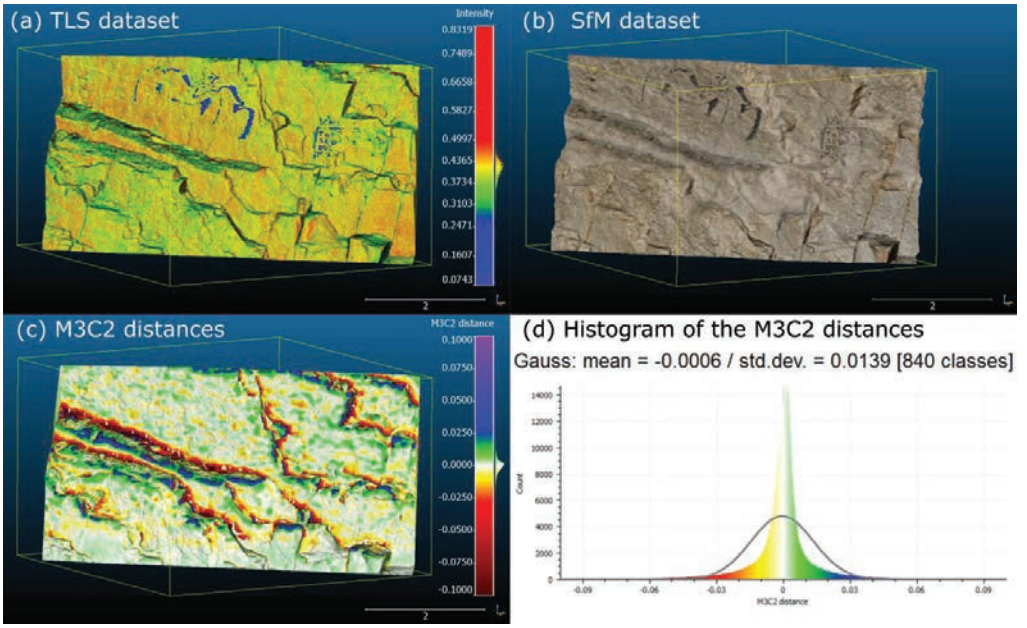

Fig. 3. (a) TLS 3DPC; (b) SfM 3DPC; (c) M3C2 distance; (d) Histogram of the M3C2 distances.

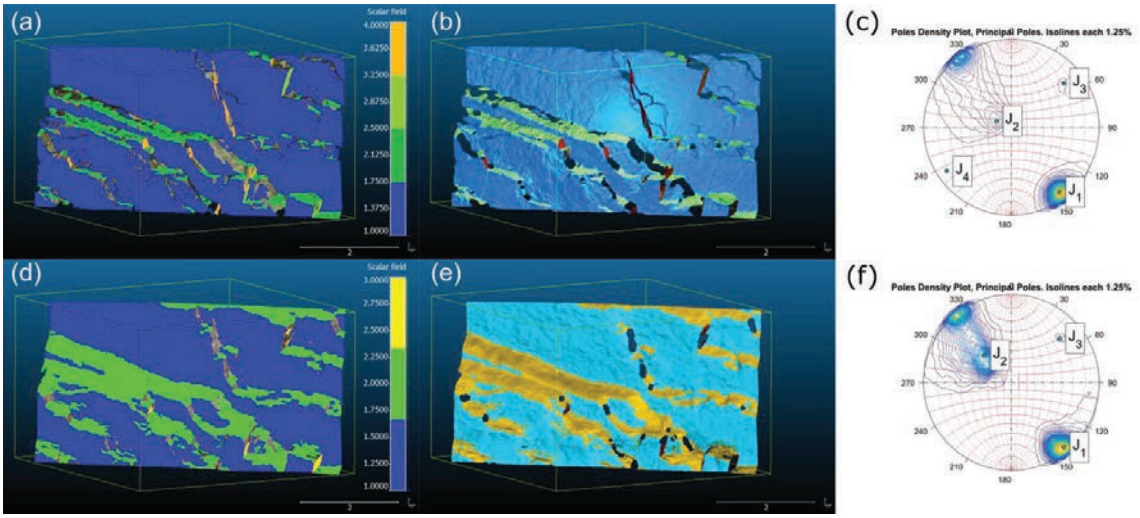

Fig. 4. Classification of the discontinuity sets of the TLS dataset (a-b) and SfM dataset (d-e); density of the normal vector's poles of the TLS.

Table 2. Discontinuity sets extracted from the TLS and SfM point clouds.

TLS dataset				SfM dataset			
Dip dir [º]	Dip [º]	Density	% of points	Dip dir [º]	Dip [º]	Density	% of points
323.41	85.13	13.87	71.46	321.08	86.94	8.59	60.27
113.13	20.53	1.15	10.24	135.05	47.15	3.15	31.29
230.01	75.67	0.25	1.46	227.67	73.09	0.13	0.87
55.89	83.40	0.09	2.02				

4. Results

On the one hand, the 3D point cloud obtained by means of the TLS consists of three dense 3D point clouds acquired from three different stations (Fig. 1c). Those three point clouds were aligned, obtaining a superposition of points equal to 12 pts cm^{-2} (Fig. 3a). On the other hand, the SfM process was performed. Once the point cloud is generated, 6 GPCs are used to georeference it using a 7 parameters rigid transformation (translation, rotation and escalation). However, this process do not compensate non-linear deformations, and camera parameters must be optimized in order to minimize the sum of reprojection error and reference coordinate misalignment error [23]. The root mean square error (RMSE) is shown in Table 1. The generated point cloud had a density equal to 2.4 pts cm^{-2} (Fig. 3b).

4.1. Point to point distance between TLS and SfM point clouds.

Fig. 3c shows the relationship between the two point clouds using the Multiscale Model to Model Cloud Comparison (M3C2) [26], which is available in the software CloudCompare [24]. The reference point cloud was the one acquired by the TLS instrument. The used processing parameters were those default by the software. Fig. 3d shows the summary statistics for all distances. This distribution has a mean value equal to 0.6 mm and a standard deviation equal to 13.9 mm.

4.2. Discontinuity set extraction of TLS and SfM point clouds.

Both TLS and SfM datasets were analyzed separately by means of the software DSE. The density of points of the SfM dataset resulted equal to 2.4 pts cm^{-2}, which is fair enough for processing the point cloud with the software. Contrarily, the point density of the TLS dataset was equal to 12 pts cm^{-2}. This sector is originally composed by more than two million and a half points, what leads to difficulties in the geometrical analysis of the points with DSE. Consequently, the TLS dataset was subsampled, setting the minimum distance between points equal to 5 mm. The parameters used in the analysis were:

- Normal vector calculation
  - knn (number of nearest neighbours) = 30
  - η (parameter of the coplanarity test, see [4]) = 20 %
- Principal poles calculation:
  - Number of bins for the density analysis: 64
  - Minimum angle between principal poles: 10º
- Assignation of points to a principal pole:
  - Maximum angle between a pole and its corresponding principal pole: 30º
- Cluster analysis:
  - Minimum number of points per cluster: 100

Statistical analysis results of the TLS and SfM datasets are shown in Fig 4c and Fig. 4f respectively. The analysis of the TLS density function leads to the identification of four discontinuity sets, and the corresponding analysis of the SfM density function identified three discontinuity sets. Table 2 illustrates the orientations of the discontinuity

sets corresponding to the analyzed datasets. According to this data, Fig. 4a shows the points of the TLS dataset classified and coloured depending on its corresponding discontinuity set. Then, a mesh was generated and Fig. 4b shows the classification including the roughness perception of the dataset. Concerning the SfM dataset, the same results are showed in Fig. 4d and e.

5. Discussion

In the previous section the obtained SfM dataset was shown. Despite Table 1 shows that the total error of the SfM process was minor than 3 mm, the visual inspection of this dataset and the TLS dataset (Fig. 4e and b respectively) founds some differences concerning the surface details. It can be observed that when using TLS technique, the surface seems to be more accurate than when using SfM technique. However, this statement must be considered with caution, as the SfM technique may lead to different results when the number of captured images increases or even when using aerial platforms, such as Remotely Piloted Aerial Systems (RPAS).

Another important finding was that comparing TLS and SfM datasets showed a good correlation of points when the surface is sub-vertical and orthogonal to the visual line or to the laser beam. On the contrary, edges and oblique surfaces showed a bad correlation (red and blue values in Fig. 3c). These findings support the idea that TLS datasets provide more reliability than SfM datasets, in terms of geometry when the digital pictures are captured under the present conditions.

An initial objective of this work was to extract discontinuity sets using both TLS and SfM techniques. As Table 2, Fig. 4c and Fig. 4f and shows, there is a significant correspondence between the discontinuity sets number 1, 2 and 3. Contrarily, using SfM dataset no statistical evidence of the existence of the discontinuity set number 4 was found.

6. Conclusions

The main goal of the present work is to determine, on the one hand, the reliability of using printed targets scanned by means of TLS instruments and added to the SfM process, and on the other hand, the extraction of discontinuity sets when using these datasets. One of the more significant findings to emerge from this study is that using GPC extracted from printed targets, which had been previously scanned by means of a TLS instrument, provides excellent results when the surface is orthogonal to the main visual direction. Unfortunately, this study has also shown that sub-horizontal and oblique surfaces are inaccurate when using SfM technique. Nevertheless, a number of important limitations need to be considered: all photographs were captured standing on the ground and the used camera was a common instrument. Therefore, there is a definite need for using Remotely Piloted Aircraft Systems (RPAS) when capturing.

Another purpose of the current study was the extraction of discontinuity sets using both datasets. The most obvious finding to emerge from this work is that, using datasets generated by the SfM technique, well exposed planes were correctly extracted. Contrarily, when planes or surfaces were not enough planar, it was found a discrepancy between those results obtained using TLS and SfM datasets. Notwithstanding these limitations, this work suggests that the use of SfM technique combined with TLS instruments presents a great potential for extracting geometrical information of rock slopes.

Acknowledgements

This work was partially funded by the University of Alicante (vigrob-157 Project and GRE 14-04 Project), the Generalitat Valenciana (Projects GV/2011/044 and ACOMP/2014/136), the Spanish Ministry of Economy and Competitiveness (MINECO) and EU FEDER under Project TIN2014-55413-C2-2-P. The 3D laser scanner used in this work for the 3D point cloud acquisition was acquired under the framework of the Programa Objetivo FEDER 2007-2013 Generalitat Valenciana - Unión Europea - Universidad de Alicante. The last author was founded by a H2020 Marie Curie Intra European Fellowship.

References

[1] S. Slob, A.K. Turner, J. Bruining, H. Hrgk, Automated rock mass characterisation using 3-D terrestrial laser scanning, TU Delft, Delft University of Technology, 2010, doi:0166077.

[2] A. Abellán, M.H. Derron, M. Jaboyedoff, 'Use of 3D Point Clouds in Geohazards' Special Issue: Current Challenges and Future Trends, Remote Sens. 8 (2016) 130.

[3] A.M. Ferrero, G. Forlani, R. Roncella, H.I. Voyat,. Advanced geostructural survey methods applied to rock mass characterization, Rock Mech. Rock Eng. 42 (2009) 631–665.

[4] A. Riquelme, A. Abellán, R. Tomás, M. Jaboyedoff, A new approach for semi-automatic rock mass joints recognition from 3D point clouds, Comput. Geosci. 68 (2014) 38–52.

[5] T.J.B. Dewez, D. Girardeau-Montaut, C. Allanic, J.F. Rohmer, A CloudCompare plugin to extract geological planes from unstructured 3D point clouds, ISPRS - Int. Arch. Photogramm. Remote Sens Spat. Inf. Sci. XLI-B5 (2016) 799–804.

[6] X. Leng, J. Xiao, Y. Wang, A multi-scale plane-detection method based on the Hough transform and region growing, Photogramm. Rec. 31 (2016) 166–192.

[7] J. Chen, H. Zhu, X. Li, Automatic extraction of discontinuity orientation from rock mass surface 3D point cloud, Comput. Geosci. 95 (2016) 18–31.

[8] R.K. Gomes, L.P.L. de Oliveira, L. Gonzaga, F.M.W. Tognoli, M.R. Veronez, M.K. de Souza, An algorithm for automatic detection and orientation estimation of planar structures in LiDAR-scanned outcrops, Comput. Geosci. 90 (2016) 170–178.

[9] A. Riquelme, A. Abellán, R. Tomás, Discontinuity spacing analysis in rock masses using 3D point clouds, Eng. Geol. 195 (2015) 185–195.

[10] A. Riquelme, R. Tomas, A. Abellán, M. Cano, M. Jaboyedoff, Semi-automatic characterization of fractured rock masses using 3D point clouds: discontinuity orientation, spacing and SMR geomechanical classification, EGU Gen. Assem. Conf. Abstr. 17 (2015) 15459.

[11] M. Sturzenegger, D. Stead, D. Elmo, Terrestrial remote sensing-based estimation of mean trace length, trace intensity and block size/shape, Eng. Geol. 119 (2011) 96–111.

[12] A. Riquelme, M. Cano, R. Tomás, A. Abellán, Using open-source software for extracting geomechanical parameters of a rock mass from 3D point clouds: Discontinuity Set Extractor and SMRTool, in: R. Ulusay, Ö. Aydan, H. Gerçek, M. Hindistan, E. Tuncay (Eds.), Rock Mech. Rock Eng. From Past to Futur. 2, 2016, pp. 1091–1096.

[13] P. Lai, C. Samson, P. Bose, Surface roughness of rock faces through the curvature of triangulated meshes, Comput. Geosci. 70 (2014) 229-237.

[14] M.R. James, S. Robson, Straightforward reconstruction of 3D surfaces and topography with a camera: Accuracy and geoscience application, J. Geophys. Res. Earth Surf. 117 (2012).

[15] A. Riquelme, R. Tomás, A. Abellán, Characterization of rock slopes through slope mass rating using 3D point clouds, Int. J. Rock Mech. Min. Sci. 84 (2016) 165–176.

[16] C. Megías, H. Corbí, A. Ramos-Esplá, A. Izquierdo-Munoz, E. Rubio, A. Abellán, et al., Methodology proposal for the sedimentological characterization of beaches in El Cabo de Santa Pola (Alicante), V Simp. Int. Ciencias del Mar, Universidad de Alicante, Alicante, 2016.

[17] A. Riquelme, A. Abellán, R. Tomás, M. Jaboyedoff, Rock slope discontinuity extraction and stability analysis from 3D point clouds: application to an urban rock slope, Vert. Geol. from Remote Sens. to 3D Geol. Model. Proc. first Vert. Geol. Conf., Univ. Lausanne, Switzerland, 2014, pp. 3-6.

[18] G. Leret Verdú, A. Lendínez González, MAGNA 50 (2 Serie) - Geological map of Spain (in Spain Mapa Geològico de España a escala) 1:50.000, hoja 872, Alicante, 1978.

[19] M. Lato, M.S. Diederichs, D.J. Hutchinson, Bias correction for view-limited Lidar scanning of rock outcrops for structural characterization, Rock Mech. Rock Eng. 43 (2010) 615–628.

[20] M.R. James, S. Robson, Mitigating systematic error in topographic models derived from UAV and ground-based image networks, Earth Surf. Process. Landforms 39 (2014)1413–1420.

[21] L.L.C. Agisoft, Image Capture Tips: Equipment and Shooting Scenarios 3, 2016.

[22] Leica. Cyclone v9.1 2016.

[23] L.L.C. Agisoft, AgiSoft PhotoScan Professional edition, AgiSoft LLC 2016.

[24] D. Girardeau-Montaut, CloudCompare (version 2.8) [GPL software], OpenSource Proj 2016.

[25] A. Riquelme, A. Abellán, R. Tomás, M. Jaboyedoff, Discontinuity Set Extractor 2014.

[26] D. Lague, N. Brodu, J.J. Leroux, Accurate 3D comparison of complex topography with terrestrial laser scanner: Application to the Rangitikei canyon (NZ), ISPRS J. Photogramm. Remote Sens. 82 (2013) 10–26.